ASTRONOMY
AND
ASTROPHYSICS

Metallicity-dependent effective temperature determination for eclipsing binaries from synthetic $uvby$ Strömgren photometry

E. Lastennet[1,2,*], T. Lejeune[1], P. Westera[1], and R. Buser[1]

[1] Astronomisches Institut der Universität Basel, Venusstrasse 7, CH-4102 Binningen, Switzerland
[2] UMR CNRS 7550, Observatoire Astronomique, 11, rue de l'Université, F-67000 Strasbourg, France

Abstract. Strömgren synthetic photometry from an empirically calibrated grid of stellar atmosphere models has been used to derive the effective temperature of each component of double lined spectroscopic (SB2) eclipsing binaries. For this purpose, we have selected a sub-sample of 20 SB2s for which (b−y), m_1, and c_1 individual indices are available. This new determination of effective temperature has been performed in a homogeneous way for all these stars. As the effective temperature determination is related to the assumed metallicity, we explore simultaneous solutions in the (T_{eff},[Fe/H])-plane and present our results as confidence regions computed to match the observed values of surface gravity, (b−y), m_1, and c_1, taking into account interstellar reddening. These confidence regions show that previous estimates of T_{eff} are often too optimistic, and that [Fe/H] should not be neglected in such determinations. Comparisons with Ribas et al. (1998) using Hipparcos parallaxes are also presented for 8 binaries of our working sample, showing good agreement with the most reliable parallaxes. This point gives a significant weight to the validity of the BaSeL models for synthetic photometry applications.

Key words: stars: binaries: eclipsing – stars: fundamental parameters – stars: statistics

1. Introduction

Fundamental stellar parameters such as masses and radii of well detached double-lined spectroscopic eclipsing binaries can be determined very accurately (Andersen 1991). Therefore, from accurate (1-2%) stellar mass and radius determinations of such objects, one can compute surface gravities to very high and otherwise inaccessible confidence levels. Indeed, Henry & Mc Carthy (1993) have discussed the data available for visual binaries of solar mass and below. Only α Cen B (G2V,0.90 M$_\odot$) has a mass known with an accuracy comparable to that for favorable eclipsing binaries. This point shows the importance of choosing such double-lined eclipsing binaries in order to obtain surface gravities with the highest possible accuracy. Moreover,

these binaries are of great interest to perform accurate tests of stellar evolutionary models (see e.g. Lastennet et al. 1996, Pols et al. 1997, Lastennet & Valls-Gabaud 1998) used to derive cluster ages. The knowledge of all possible stellar parameters for such single stars is the basis of the modelling of the global physical properties and evolution of star clusters or galaxies. Nevertheless, while masses and radii are accurately known, the effective temperatures – and consequently, the luminosities of these stars – strongly depend upon the calibration used to relate photometric indices with T_{eff}. As a matter of fact, for such binaries the temperatures given in the literature come from various calibration procedures and are indeed highly inhomogeneous. Furthermore, due to the lack of empirical calibrations at different metallicities, solar metallicity is often assumed for photometric estimations of T_{eff}. In this regard, synthetic photometry performed from large grids of stellar atmosphere models, calibrated in T_{eff}, $\log g$, and [Fe/H], provides a powerful tool of investigation. In this paper, we explore simultaneous solutions of T_{eff} and [Fe/H], and we address the question of the reliability of metallicity-independent effective temperature determinations.

We have selected 20 binary systems (40 stars) for which we have $uvby$ Strömgren photometry with estimated errors (see Table 1). For this sample, previous estimates of effective temperature are not homogeneous, originating from various calibrations established for different spectral-type domains: Morton & Adams (1968), Relyea & Kurucz (1978), Osmer & Peterson (1974), Grosbøl (1978), Davis & Shobbrook (1977), Popper (1980), Moon & Dworetsky (1985), Saxner & Hammarbäck (1985), Jakobsen (1986), Magain (1987), Napiwotzki et al. (1993), and Edvardsson et al. (1993). Moreover, all these studies are of course historically not fully independent. As an example, the T_{eff} of Moon & Dworetsky (1985) is estimated using the T_{eff}, (B−V)$_0$ calibration of Hayes (1978) and the T_{eff}, c$_0$ calibration of Davis & Shobbrook (1977). However, this does not mean that these calibrations allow to derive very similar temperatures. As highlighted by Andersen & Clausen (1989) concerning the O-type components of EM Carinae, the temperature calibration of Davis & Shobbrook (1977), Jakobsen (1986), and Popper (1980) do not agree particularly well. A similar comparison of these three calibrations made by Clausen & Giménez (1991) with the massive B-type components of CW Cephei leads to $\Delta T_{eff} \sim 5500$K ! Thus, a new *and* homogeneous

determination of effective temperature is of primordial interest for such well-known objects. In order to re-derive in a homogeneous way the T_{eff} of these stars, we have used the *Ba*sel *Ste*llar *Li*brary (hereafter *"BaSeL"*) which provides empirically calibrated model spectra over a large range of stellar parameters (Lejeune et al. 1997, 1998a).

In Sect. 2, we will describe the models used to perform our calculation of T_{eff} from *uvby* Strömgren photometry. Sect. 3 will be devoted to the description of the method and the presentation of the results.

2. Model colours

The BaSeL models cover a large range of fundamental parameters: $2000\,\mathrm{K} \leq T_{\mathrm{eff}} \leq 50{,}000\,\mathrm{K}$, $-1.02 \leq \log g \leq 5.5$, and $-5.0 \leq [\mathrm{M/H}] \leq +1.0$. This library combines theoretical stellar energy distributions which are based on several original grids of blanketed model atmospheres, and which have been corrected in such a way as to provide synthetic colours consistent with extant empirical calibrations at all wavelengths from the near-UV through the far-IR (see Lejeune et al. 1997, 1998a). For our purpose, we have used the new version of the BaSeL models for which the correction procedure of the theoretical spectra has been extended to higher temperatures ($T_{\mathrm{eff}} \geq 12{,}000$ K), using the T_{eff}–(B−V) calibration of Flower (1996), and to shorter wavelengths (Lejeune et al. 1998b). Because the correction procedure implies modulations of the (pseudo-)continuum which are smooth between the calibration wavelengths, the final grid provides colour-calibrated flux distributions ($9.1 \leq \lambda \leq 160{,}000$ nm, with a mean resolution of $1 \sim 2$ nm from the UV to the visible) which are also suitable for calculating medium-band synthetic photometry, such as Strömgren colours. Thus, synthetic Strömgren photometry was performed using the passband response functions (u, v, b, y) given in Schmidt-Kaler (1982). Theoretical (u−b), (b−y), $m_1 = (v-b)-(b-y)$, and $c_1 = (u-v)-(v-b)$ indices have been computed, where the zero-points were defined by matching the observed colours (u−b = 1.411, b−y= 0.004, $m_1 = 0.157$, $c_1 = 1.089$; Hauck & Mermilliod 1980) of Vega with those predicted by the corresponding Kurucz (1991) model for $T_{\mathrm{eff}} = 9400$ K, $\log g = 3.90$, [M/H] $= -0.50$.

3. Effective temperature determination

3.1. Strömgren data

Among the approximately sixty SB2 systems gathered in Lastennet (1998), only 20 have both individual *uvby* Strömgren photometric indices and uncertainties for each component. Uncertainties are a key point in the calculation presented later (Sect. 3.2). The photometry used for the 20 systems of our working sample (see Table 1) is from the recent Table 5 of Jordi et al. (1997), who have taken the individual indices directly from the literature but have also added their own results for three systems (YZ Cas, WX Cep, and IQ Per).
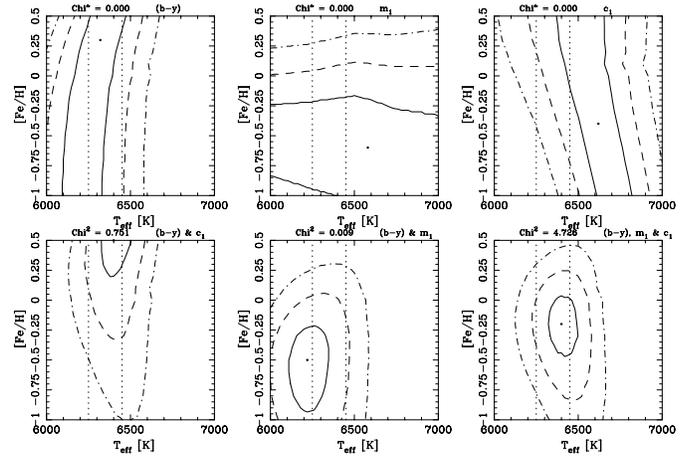
Fig. 1. Simultaneous solutions of T_{eff} and [Fe/H] for BW Aqr A (assuming $\log g = 3.981$): matching (b−y) (*upper left*), m_1 (*upper central*), c_1 (*upper right*), (b−y), and c_1 (*lower left*), (b−y), and m_1 (*lower central*), (b−y), m_1, and c_1 (*lower right*). Best fit (*black dot*) and 1-σ (*solid line*), 2-σ (*dashed line*), and 3-σ (*dot-dashed line*) confidence levels are also shown. Previous estimates of T_{eff} from Clausen (1991) are indicated as vertical dotted lines in all panels.

3.2. Methodology

To compute synthetic colours from the BaSeL models, we need effective temperature (T_{eff}), surface gravity ($\log g$), and metallicity ([Fe/H]). Consequently, given the observed colours (namely, b−y, m_1, and c_1), we are able to derive T_{eff}, $\log g$, and [Fe/H] from a comparison with model colours. As the surface gravities can be derived very accurately from the masses and radii of the stars in our working sample, only two physical parameters have to be derived (T_{eff} and [Fe/H]).

This has been done by minimizing the χ^2-functional, defined as

$$\chi^2(T_{\mathrm{eff}}, [Fe/H]) = \sum_{i=1}^{n} \left[\left(\frac{\mathrm{colour(i)_{syn}} - \mathrm{colour(i)}}{\sigma(\mathrm{colour(i)})} \right)^2 \right], (1)$$

where n is the number of comparison data, colour(1)= $(b-y)_0$, colour(2)= m_0, and colour(3) = c_0. The best χ^2 is obtained when the synthetic colour, colour(i)$_{\mathrm{syn}}$, is equal to the observed one.

Reddening has been taken into account following Crawford (1975): $(b-y)_0 = (b-y) - \mathrm{E}(b-y)$, $m_0 = m_1 + 0.3 \times \mathrm{E}(b-y)$, $c_0 = c_1 - 0.2 \times \mathrm{E}(b-y)$, in order to derive the intrinsic colours from the observed ones. With $n = 3$ observational data (b−y, m_1, c_1) and $p = 2$ free parameters (T_{eff} and [Fe/H]), we expect to find a χ^2-distribution with $q = n - p = 1$ degree of freedom. Finding the central minimum value χ^2_{min}, we form the χ^2-grid in the (T_{eff}, [Fe/H])-plane and compute the boundaries corresponding to 1 σ, 2 σ, and 3 σ respectively. As our sample contains only stars belonging to the Galactic disk, we have explored a restricted range of metallicity, $-1.0 \leq [\mathrm{Fe/H}] \leq +0.5$.

Fig. 1 illustrates the different steps of the method, here for BW Aqr A. All possible combinations of observational data (as indicated on the top of each panel) are explored, hence varying the number of degrees of freedom for minimizing the χ^2. The

Table 1. Strömgren photometry for the sample (after Table 5 of Jordi et al. 1997). Some useful notes about reddening are given in the last column.

| System	(b−y)	m_1	c_1	$\log g$	E(b−y)[†]	E(b−y)
BW Aqr	0.345±0.015	0.15±0.03	0.45±0.03	3.981±0.020	0.03	0.03 [a]
	0.325±0.015	0.16±0.03	0.45± 0.03	4.075±0.022	0.03	0.03 [a]
AR Aur	−0.043±0.010	0.142±0.012	0.857± 0.015	4.331±0.025	0.	0. [z]
	−0.021±0.010	0.162±0.012	0.892±0.015	4.280±0.025	0.	0. [z]
β Aur	−0.003±0.026	0.162±0.053	1.124±0.057	3.930±0.010	0.	0. [z]
	0.005±0.026	0.206±0.053	1.121±0.057	3.962±0.010	0.	0. [z]
GZ Cma	0.077±0.010	0.193±0.020	1.066±0.025	3.989±0.012	0.047	0.047±0.02 [b]
	0.091±0.010	0.216±0.020	1.002±0.025	4.083±0.016	0.047	0.047±0.02 [b]
EM Car	0.310±0.010	−0.038±0.010	−0.089±0.010	3.857±0.017	0.44	0.44 [c]
	0.310±0.010	−0.047±0.010	−0.076±0.010	3.928±0.016	0.44	0.44 [c]
YZ Cas	0.004±0.006	0.186±0.009	1.106±0.011	3.995±0.011	0.	0. [z]
	0.248±0.081	0.196±0.166	0.309±0.238	4.309±0.010	0.	0. [z]
WX Cep	0.330±0.007	0.105±0.012	1.182±0.023	3.640±0.011	0.3	0. [z]
	0.271±0.022	0.080±0.036	1.190±0.060	3.939±0.011	0.3	0. [z]
CW Cep	0.333±0.010	−0.071±0.015	0.037±0.015	4.059±0.024	0.46	0.46 [d]
	0.339±0.010	−0.064±0.015	0.045±0.015	4.092±0.024	0.46	0.46 [d]
RZ Cha	0.314±0.016	0.149±0.027	0.480±0.027	3.909±0.009	0.003	0. [z]
	0.304±0.017	0.165±0.029	0.468±0.029	3.907±0.010	0.003	0. [z]
KW Hya	0.105±0.005	0.243±0.007	0.919±0.005	4.079±0.013	0.01	0. [e,z]
	0.244±0.011	0.210±0.007	0.490±0.047	4.270±0.010	0.01	0. [e,z]
GG Lup	−0.049±0.007	0.097±0.011	0.450±0.012	4.301±0.012	0.020	0.020 [f]
	−0.019±0.019	0.141±0.032	0.811±0.036	4.364±0.010	0.020	0.020 [f]
TZ Men	−0.025±0.007	0.140±0.010	0.941±0.010	4.225±0.011	0.	0. [z]
	0.185±0.007	0.176±0.015	0.689±0.015	4.303±0.009	0.	0. [z]
V451 Oph	0.084±0.010	0.083±0.020	0.940±0.020	4.038±0.015	0.115	0.115 [g]
	0.103±0.010	0.109±0.020	0.992±0.020	4.196±0.015	0.115	0.115 [g]
V1031 Ori	0.10±0.01	0.17±0.02	1.13±0.03	3.560±0.008	0.05	0. [h]
	0.05±0.01	0.16±0.02	1.13±0.03	3.850±0.019	0.05	0. [h]
IQ Per	0.056±0.004	0.079±0.005	0.635±0.011	4.208±0.019	0.11	0.10±0.01 [i]
	0.165±0.049	0.089±0.103	0.819±0.186	4.323±0.013	0.11	0.10±0.01 [i]
AI Phe	0.528±0.010	0.308±0.010	0.379±0.010	3.593±0.003	0.015	0.015±0.02 [j]
	0.316±0.010	0.172±0.010	0.421±0.010	4.021±0.004	0.015	0.015±0.02 [j]
ζ Phe	−0.07±0.02	0.13±0.03	0.49±0.03	4.122±0.009	0.	0. [z]
	−0.01±0.02	0.11±0.03	0.77±0.03	4.309±0.012	0.	0. [z]
PV Pup	0.201±0.024	0.171±0.041	0.628±0.041	4.257±0.010	0.06	0. [z]
	0.201±0.025	0.159±0.043	0.640±0.043	4.278±0.011	0.06	0. [z]
VV Pyx	0.016±0.006	0.156±0.010	1.028±0.010	4.089±0.009	0.016	0.016 [k]
	0.016±0.006	0.156±0.010	1.028±0.010	4.088±0.009	0.016	0.016 [k]
DM Vir	0.317±0.007	0.171±0.010	0.480±0.012	4.108±0.009	0.017	0.017 [l]
	0.317±0.007	0.171±0.010	0.480±0.012	4.106±0.009	0.017	0.017 [l]

[†] this work (cf. Sect 3.3.2)
[a] Clausen (1991); [b] Popper et al. (1985); [c] Andersen & Clausen (1989); [d] Clausen & Giménez (1991); [e] Our value is consistent with E(b−y)=0.009±0.008 for A-stars (Crawford, 1979); [f] Andersen et al. (1993) using the $(b−y)_0−c_0$ relation of Crawford (1978); [g] Clausen et al. (1986) determined the reddening from the $[u−b]−(b−y)_0$ relation for early-type stars of Strömgren & Olsen (unpublished) and the $c_0−(b−y)_0$ relation of Crawford (1973), which give nearly identical results; [h] Andersen et al. (1990) used E(b−y)= 0.0 but quote E(b−y)=0.025 as a possible value; [i] E(B−V)=0.14±0.01 (Lacy & Frueh 1985); [j] E(B−V)=0.02±0.02 (Hrivnak & Milone 1984); [k] Andersen et al. (1984) using the calibrations of Grosbøl (1978); [l] Moon & Dworetsky (1985); [z] At the best of our knowledge, systems for which interstellar reddening has been neglected or considered as insignificant in the literature.
Note: we assume E(b−y)=0.73×E(B−V) after Crawford (1975).

top panels show the results obtained for matching uniquely one colour index (b−y, m_1, or c_1). In these cases, $q = n − p = -1$, which simply means that it is impossible to fix both T_{eff} and [Fe/H] with only one observational quantity, as indeed is illustrated by the three top panels of Fig. 1. From (b−y) only, the effective temperature boundaries appear to be very similar across the whole metallicity range, highlighting the fact that this index is traditionally used to derive T_{eff}. Alternatively, the m_1
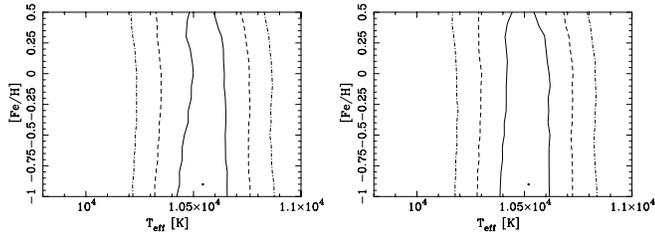
Fig. 2. Influence of $\log g$ on the simultaneous solution of T_{eff} and [Fe/H] for AR Aur B. Two different $\log g$ values are considered: $\log g = 4.255$ (*left panel*), $\log g = 4.305$ (*right panel*). These values are 0.025 dex higher or lower than the true $\log g$ (4.280).

index only provides constraints on the metallicity of the star. Used together (lower central panel), these two indices outline restricted "islands" of solutions in the (T_{eff}, [Fe/H])-plane, and hence offer a good combination to estimate these parameters. The c_1 index has been originally designed to estimate the surface gravity, but it also appears to be a good indicator of temperature in the parameter range explored for BW Aqr A (upper right panel). On the lower right panel, *all* the available observational information (b−y, m_1, c_1, and $\log g$) can be exploited. The range of T_{eff} values that we then derive for BW Aqr A agree well with previous estimates (as indicated by the vertical dotted lines), and the same is true for its metallicity, which is compatible with the Galactic disk stars. Finally, in order to take full advantage of all the observational information available for the stars in our sample, we choose to estimate T_{eff} and [Fe/H] from a χ^2 minimization performed on the three colour indices.

3.3. Surface gravity accuracy and influence of reddening

3.3.1. Surface gravity

As our results depend not only on the accuracy of the photometric data, but also on that of the surface gravity determination, we analysed the effect of a variation of $\log g$ upon the predicted T_{eff} and [Fe/H] values. We investigated this "$\log g$ effect" for the AR Aur system, for which the known value of $\log g$ has the largest uncertainties in our working sample: for instance, the surface gravity of the coolest component of AR Aur (AR Aur B) is $\log g = 4.280 \pm 0.025$.

For $\log g = 4.280$, the central T_{eff} value predicted is about 10,500K. If we consider $\log g - 0.025$ dex (left panel in Fig. 2) or $\log g + 0.025$ dex (right panel in Fig. 2), neither the central T_{eff} value nor the pattern of contours change significantly.

This example shows that our results for (T_{eff},[Fe/H]) will not change due to variations of surface gravity within the errors listed in Table 1.

3.3.2. Interstellar reddening

Interstellar reddening is of prime importance for the determination of both T_{eff} and [Fe/H]. A great deal of attention was therefore devoted to the E(b−y) values available in the literature, for each star of our sample. We explore different reddening
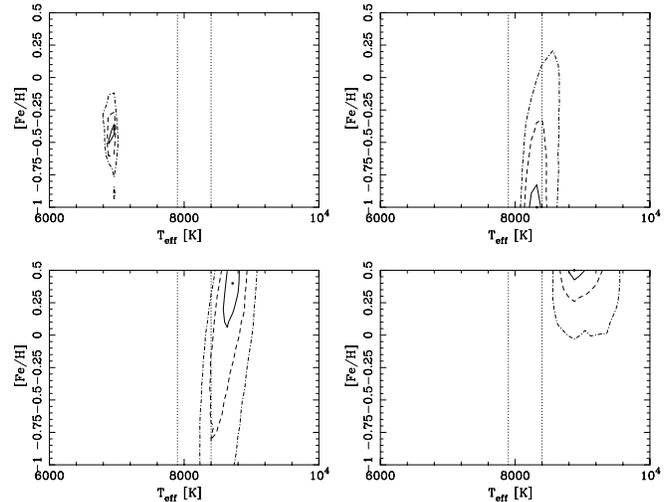
Fig. 3. Influence of reddening on the simultaneous solutions of T_{eff} and [Fe/H] for WX Cep A. Different reddening values are considered: E(b−y) = 0.00 (*upper left*), E(b−y) = 0.30 (*upper right*), E(b−y) = 0.32 (*lower left*), and E(b−y) = 0.34 (*lower right*). Previous determination of T_{eff} from Popper (1987) (using Popper's 1980 calibrations) is also shown for comparison (*vertical dotted lines*).

Table 2. Influence of reddening on the χ^2 of the components of the WX Cephei system. Best χ^2 are in bold characters. The hypothesis of no reddening is definitively ruled out.

E(b−y)	WX Cep A χ^2-values	WX Cep B χ^2-values
0.00	912.890	115.290
0.26	29.039	0.933
0.28	10.974	**0.682**
0.30	4.549	1.210
0.32	**4.009**	2.651
0.34	4.322	4.972

values (as described in Sect. 3.2), and we compare their resulting χ^2-scores. For the following systems, we adopted the published values, in perfect agreement with our results: BW Aqr, AR Aur, β Aur, GZ Cma, EM Car, CW Cep, GG Lup, TZ Men, V451 Oph, AI Phe, ζ Phe, VV Pyx, and DM Vir. As we did not find any indication about the interstellar reddening of YZ Cas, we kept E(b−y) = 0 as a quite reasonable hypothesis. We have neither found any data on interstellar reddening for the WX Cephei system. But the hypothesis of no significant reddening for WX Cep is ruled out by the very high χ^2-value obtained in reproducing simultaneously the quadruplet (b−y, m_1, c_1, $\log g$) of the observed data. From the different reddening values explored in Table 2, we find that E(b−y) = 0.32 for WX Cep A and E(b−y) = 0.28 for WX Cep B provide the best solutions.

The influence of reddening variations is illustrated in Fig. 3. While for the system, WX Cep AB, an average value E(b−y) = 0.30 appears justified from the results of Table 2 – and will indeed be adopted in the remainder of this paper –, Fig. 3 shows how for the individual component, WX Cep A, small changes

ΔE(b$-$y)= $\pm$0.02 away from its own optimum value E(b$-$y) = 0.32 induce significant changes in the possible solutions of the ($T_{\rm eff}$, [Fe/H])-couples. In particular, going to E(b$-$y) = 0.30 (upper right panel) implies a dramatic jump in predicted [Fe/H] from a (plausible) metal-normal (lower left) to a (rather unlikely?) metal-poor composition at or near the lower limit ([Fe/H] = -1) of the exploration range.

For the other four systems for which interstellar reddening has also been previously neglected in the literature, we found small, but not significant, E(b$-$y) values: RZ Cha (0.003), KW Hya (0.01), V1031 Ori (0.05), and PV Pup (0.06).

E(b$-$y) = 0.11 has been adopted for IQ Per by comparing different $\chi^2_{\rm min}$ solutions. This value is consistent with E(b$-$y) = 0.10$\pm$0.01, estimated from the published value of E(B$-$V) = 0.14$\pm$0.01 (Lacy & Frueh 1985), assuming E(b$-$y) = 0.73$\times$E(B$-$V) after Crawford (1975). Adopted reddening values for stars of our sample are listed in Table 1.

3.4. General results and discussion

In Figs. 4 and 5 we show the full results obtained (from b$-$y, m_1, and c_1) for all the stars of the sample in ($T_{\rm eff}$, [Fe/H]) planes. All the ($T_{\rm eff}$,[Fe/H])-solutions inside the contours allow to reproduce, at different confidence levels, both the observed Strömgren colours (b$-$y, m_1, and c_1) and the surface gravity with the BaSeL models. As a general trend, it is important to notice that our $T_{\rm eff}$ ranges do not provide estimates systematically different from previous ones (vertical dotted lines). Furthermore, the 3-σ confidence regions show that most previous $T_{\rm eff}$ estimates are optimistic, except for some stars (e.g., GG Lup A, TZ Men A, and V451 Oph A) for which our method gives better constraints on the estimated effective temperature. At a 1-σ confidence level (68.3%), our method often provides better constraints for $T_{\rm eff}$ determination. However, it is worth noticing that for a few stars the match is really bad (see $\chi^2_{\rm min}$-values labelled directly on Fig. 4 and 5). As already mentioned, with 3 observational data (b$-$y, m_1, c_1) and 2 free parameters ($T_{\rm eff}$ and [Fe/H]), we expect to find a χ^2-distribution with 3$-$2=1 degree of freedom and a typical $\chi^2_{\rm min}$-value of about 1. For some stars (e.g. VV Pyx, DM Vir and KW Hya A), $\chi^2_{\rm min}$ is greater than 10, a too high value to be acceptable because the probability to obtain an observed minimum χ-square greater than the value χ^2=10 is less than 0.2%. For this reason, the results given for a particular star should not be used without carefully considering the $\chi^2_{\rm min}$-value.

One of the most striking features appearing in nearly all panels of Figs. 4 and 5 is the considerable range of [Fe/H] accepted inside the confidence levels. This is particularly true for stars hotter than $\sim$ 10,000 K (as, for instance, EM Car A & B and GG Lup A & B), for which optical photometry is quite insensitive to the stellar metal content. For these stars, a large range in [Fe/H] gives very similar χ^2 values. In contrast, for the coolest stars in our sample, our method provides straight constraints on their metallicity. Actually, when observational metallicity indications are available (β Aur, YZ Cas, RZ Cha, AI Phe, and PV Pup), the contour solutions are found in good agreement with previous estimated [Fe/H] ranges (labelled as horizontal lines in Figs. 4 and 5).

The effective temperatures derived from our minimization procedure cannot be easily presented in a simple table format, as they are intrinsically related to metallicity. We nonetheless provide in Table 3, as an indication of the estimated stellar parameters for all the stars in our sample, the best ($\chi^2_{\rm min}$) simultaneous solutions ($T_{\rm eff}$,[Fe/H]) for the three following cases: by using b$-$y and m_1 (Case 1), b$-$y and c_1 (Case 2) and by using b$-$y, m_1, and c_1 (Case 3). In Case 1 and Case 2, a typical $\chi^2_{\rm min}$-value close to zero is theoretically expected, and in Case 3, as previously mentioned, one expects a typical $\chi^2_{\rm min}$-value of about 1. There are quite a few stars for which $\chi^2_{\rm min}$ increases dramatically between Case 1 or 2 and Case 3 to a clearly unacceptable value (most notably AI Phe A between Case 1 and Case 3). This point means that although a good fit is obtained with two photometric indices, no acceptable $\chi^2_{\rm min}$-value is obtained by adding one more index in Case 3. Consequently, Case 1 or Case 2-solutions have to be chosen in such cases. For these stars, even if the $\chi^2_{\rm min}$ solutions shown in Figs. 4 and 5 are not reliable, it is interesting to notice that the contours derived are however still in agreement with previous works.

The surprising result in Table 3 is that many solutions are very metal-poor. This in fact means that the $\chi^2_{\rm min}$ solutions are not *necessarily* the most realistic ones. We must, therefore, emphasize that the values presented in Table 3 should not be used without carefully considering the confidence level contours shown in Figs. 4 and 5. For most stars in our sample, $T_{\rm eff}$ and [Fe/H] do not appear strongly correlated (i.e. the confidence regions do not exhibit oblique shapes), but there are a few cases for which the assumed metallicity leads to a different range in the derived effective temperature (EM Car B, CW Cep A & B, GG Lup A, ζ Phe A). These results point out that the classical derivation of $T_{\rm eff}$ from calibration without exploring all [Fe/H] values is not always a reliable method, even for hot stars.

3.5. Comparison with Hipparcos parallax

Very recently, Ribas et al. (1998) have computed the effective temperatures of 19 eclipsing binaries included in the Hipparcos catalogue from their radii, Hipparcos trigonometric parallaxes, and apparent visual magnitudes corrected for absorption. They used Flower's (1996) calibration to derive bolometric corrections. Only 8 systems are in common with our working sample. The comparison with our results is made in Table 4. The $T_{\rm eff}$ being highly related with metallicity, a direct comparison is not possible because, unlike the Hipparcos-derived data, our results are not given in terms of temperatures with error bars, but as ranges of $T_{\rm eff}$ compatible with a given [Fe/H]. Thus, the ranges reported in Table 4 are given assuming three different hypotheses: [Fe/H]= -0.2, [Fe/H] = 0, and [Fe/H] = 0.2. The overall agreement is quite satisfactory, as illustrated in Fig. 6.

The disagreement for the temperatures of CW Cephei can be explained by the large error of the Hipparcos parallax ($\sigma_\pi/\pi \simeq$70%). For such large errors, the Lutz-Kelker correction (Lutz & Kelker 1973) cannot be neglected: the average distance is
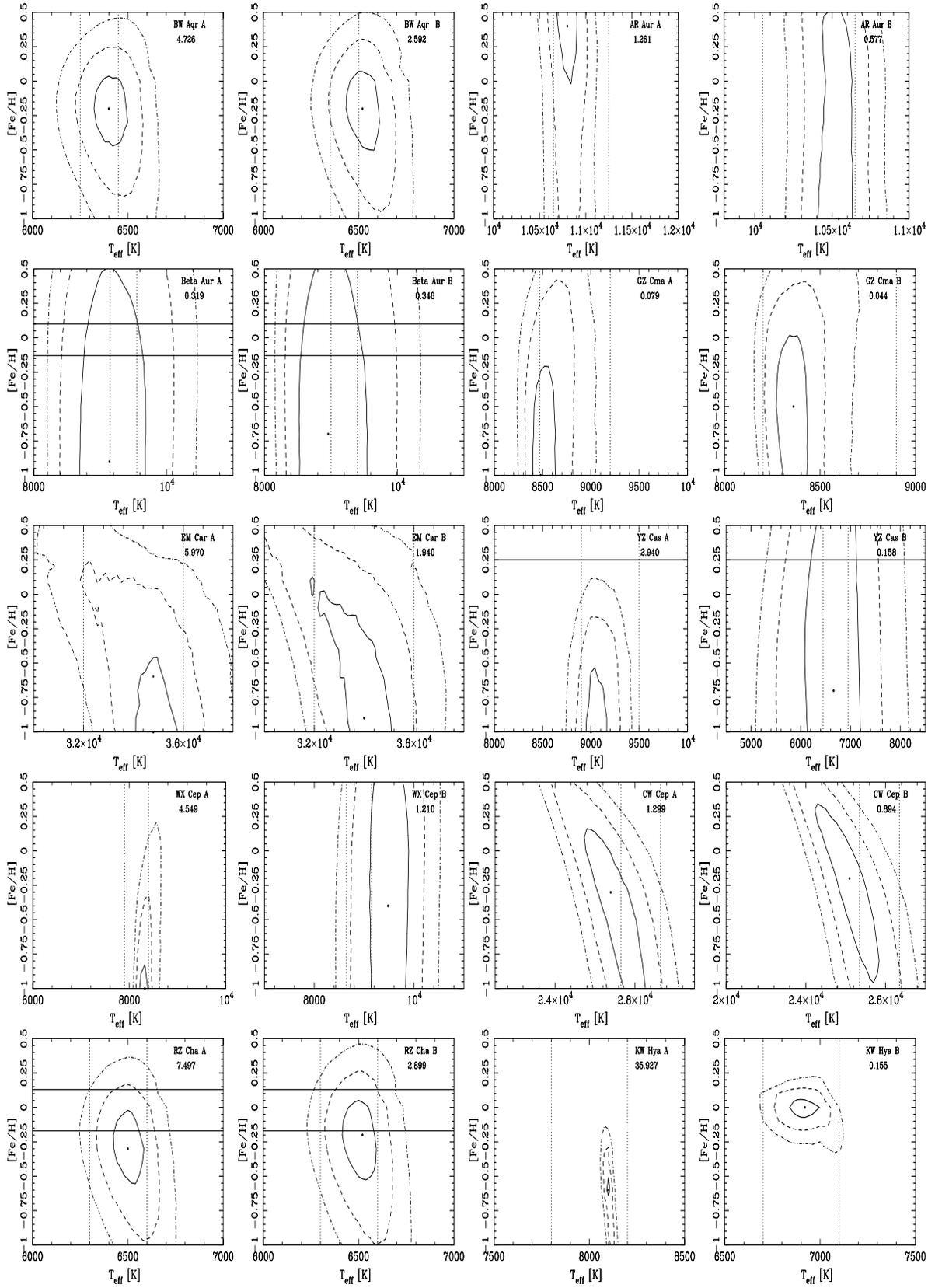
Fig. 4. Simultaneous solution of T_{eff} and [Fe/H] matching $(b-y)_0$, m_0, c_0, and $\log g$. The name of the star and the $\chi^2_{\min}$ are labelled directly in each panel. When available, effective temperature determinations from previous studies (*vertical lines*) and observational indications of metallicity (*horizontal lines*) are also shown.
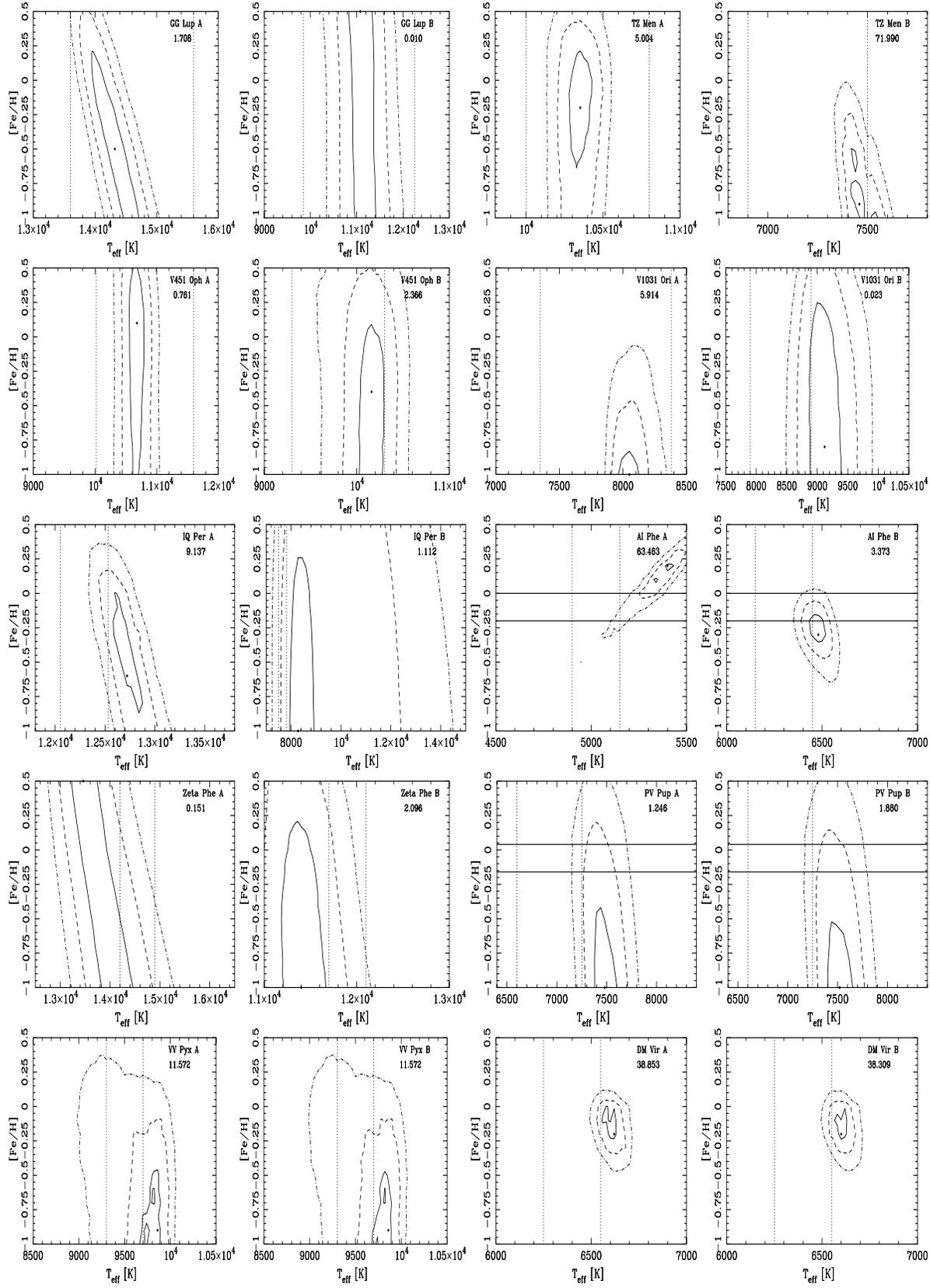
Fig. 5. Same as Fig. 4.

Table 3. Best simultaneous (T_{eff},[Fe/H]) solutions using (b−y) and m_1 (Case 1), (b−y) and c_1 (Case 2) or (b−y), m_1, and c_1 (Case 3).

| Name	Case 1			Case 2			Case 3		
	T_{eff}	[Fe/H]	$\chi^2_{\min}$	T_{eff}	[Fe/H]	$\chi^2_{\min}$	T_{eff}	[Fe/H]	$\chi^2_{\min}$
BW Aqr	6220	−0.5	0.01	6400	0.5	0.75	6400	−0.2	4.73
	6400	−0.4	0.00	6540	0.5	0.27	6520	−0.2	2.59
AR Aur	11240	0.5	0.00	10760	0.5	0.66	10800	0.4	1.26
	10352	−0.2	0.00	10568	−0.6	0.00	10544	−1.0	0.58
β Aur	9260	−0.8	0.13	9140	−0.9	0.18	9140	−0.9	0.32
	8900	0.2	0.00	9020	−1.0	0.19	8960	−0.7	0.35
GZ Cma	8480	−1.0	0.06	8480	−0.9	0.02	8480	−1.0	0.08
	8340	−0.6	0.00	8380	−1.0	0.01	8360	−0.5	0.04
EM Car	30640	−0.9	2.72	35920	0.5	0.01	34800	−1.0	5.97
	30000	−1.0	0.50	32240	0.2	0.01	34000	−0.9	1.94
YZ Cas	9080	−1.0	0.00	9000	−1.0	2.93	9000	−1.0	2.94
	6820	−0.2	0.00	6660	−1.0	0.08	6660	−0.7	0.16
WX Cep	8380	−1.0	1.57	8180	0.2	0.00	8280	−1.0	4.55
	9960	0.4	0.00	9480	−0.2	1.10	9480	−0.4	1.21
CW Cep	31000	0.4	0.00	26800	−0.3	0.01	26800	−0.3	1.30
	29400	0.5	0.25	24000	0.5	0.00	26200	−0.2	0.89
RZ Cha	6240	−0.6	0.02	6500	0.5	2.06	6500	−0.3	7.50
	6340	−0.4	0.01	6520	0.5	0.40	6520	−0.2	2.90
KW Hya	7860	−0.8	0.06	8120	−1.0	34.60	8100	−0.6	35.93
	6900	0.0	0.03	6940	0.4	0.02	6920	0.0	0.15
GG Lup	14320	−0.5	1.70	14320	−0.5	0.08	14320	−0.5	1.71
	11000	0.5	0.00	11080	0.5	0.00	11080	0.5	0.01
TZ Men	10780	−0.4	0.00	10255	0.2	0.01	10352	−0.2	5.00
	7220	−1.0	1.51	7440	0.4	43.51	7460	−0.9	71.99
V451 Oph	11160	−0.4	0.05	10620	0.3	0.05	10680	0.1	0.76
	10480	−1.0	0.63	10080	−0.8	0.25	10160	−0.4	2.37
V1031 Ori	8080	−1.0	5.62	7990	−1.0	0.06	8050	−1.0	5.91
	9120	−0.8	0.02	9120	−0.8	0.00	9120	−0.8	0.02
IQ Per	13600	−0.9	7.62	12760	−0.7	0.10	12720	−0.6	9.14
	8600	−1.0	0.88	8120	0.5	0.09	8280	−1.0	1.11
AI Phe	4860	−0.9	0.11	4860	−0.1	42.05	5400	0.2	63.46
	6360	−0.3	0.03	6420	0.3	0.01	6480	−0.3	3.37
ζ Phe	12820	0.5	0.00	13620	0.2	0.01	13460	0.5	0.15
	11000	−1.0	1.50	11400	−1.0	1.34	11400	−1.0	2.10
PV Pup	7440	−1.0	1.21	7520	−1.0	0.09	7480	−1.0	1.25
	7440	−1.0	1.71	7520	−0.5	0.01	7520	−1.0	1.88
VV Pyx	9260	−0.9	8.55	9020	0.5	0.18	9860	−0.9	11.57
	9260	−0.9	8.55	9020	0.5	0.18	9860	−0.9	11.57
DM Vir	6360	−0.3	0.15	6600	0.5	15.41	6620	−0.2	38.85
	6360	−0.3	0.15	6600	0.5	15.41	6600	−0.2	38.31

certainly underestimated and, as a consequence, the T_{eff} is also underestimated in Ribas et al.'s (1998) calculation. Thus, the agreement with the results obtained from the BaSeL models is certainly better than it would appear in Fig. 6 and Table 4. Similar corrections, of slightly lesser extent, are probably also indicated for the T_{eff} of RZ Cha and GG Lup, which have $\sigma_\pi/\pi >$ 10% (11.6% and 11.4%, respectively). Finally, it is worth noting that the system with the smallest relative error in Table 4, β Aur, shows excellent agreement between T_{eff} (Hipparcos) and T_{eff} (BaSeL), which underlines the validity of the BaSeL models.

4. Conclusion

The comprehensive knowledge of fundamental parameters of single stars is the basis of the modelling of star clusters and galaxies. Most fundamental stellar parameters of the individual components in SB2 eclipsing binaries are known with very high accuracy. Unfortunately, while masses and radii are well determined, the temperatures strongly depend on photometric calibrations. In this paper, we have used an empirically-calibrated grid of theoretical stellar spectra (BaSeL models) for simultaneously deriving homogeneous effective temperatures and metal-

Table 4. Effective temperatures from Hipparcos (after Ribas et al. 1998) and from BaSeL models matching $(b-y)_0$, m_0, c_0, and $\log g$ for the three following metallicities: $[Fe/H]= -0.2$, $[Fe/H] = 0$ and $[Fe/H] = 0.2$.

Name	T_{eff}(Hipp.) [K]	$[Fe/H]= -0.2$		$[Fe/H] = 0.$		$[Fe/H] = 0.2$	
		T_{eff}(BaSeL) [K]	σ	T_{eff}(BaSeL) [K]	σ	T_{eff}(BaSeL) [K]	σ
β Aur	9230±150	[8780,9620]	1	[8780,9560]	1	[8900,9500]	1
	9186±145	[8540,9500]	1	[8600,9440]	1	[8660,9320]	1
YZ Cas	8624±290	[9000,9120]	2	[8920,9240]	3	no solution	
	6528±155	[6100,7140]	1	[6180,7060]	1	[6260,7060]	1
CW Cep	23804	[26000,27200]	1	[25600,26600]	1	[24600,26600]	2
	23272	[25600,26800]	1	[25200 26200]	1	[24800,25400]	1
RZ Cha	6681±400	[6440,6560]	1	[6380,6600]	2	[6340,6640]	3
	6513±385	[6420,6580]	1	[6460,6540]	1	[6420,6580]	2
KW Hya	7826±340	[8080,8100]	3	no solution		no solution	
	6626±230	[6780,7120]	3	[6860,6980]	1	[6860,7000]	3
GG Lup	16128±2080	[14080,14260]	1	[14020,14140]	1	[13780,14140]	2
	12129±1960	[10920,11320]	1	[10920,11320]	1	[10920,11320]	1
TZ Men	9489±490	[10300,10420]	1	[10300,10380]	1	[10260,10460]	2
	6880±190	[7340,7460]	3	no solution		no solution	
ζ Phe	14631±1150	[13540,14020]	1	[13460,13860]	1	[13380,13860]	1
	12249±1100	[11240,11560]	1	[11280,11480]	1	[11040,11680]	2
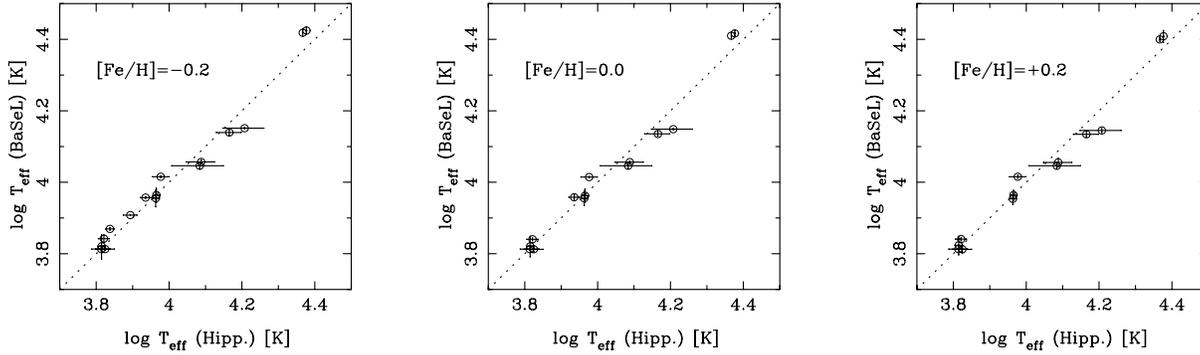
Fig. 6. Hipparcos- versus BaSeL-derived effective temperatures for β Aur, YZ Cas, CW Cep, RZ Cha, KW Hya, GG Lup, TZ Men, and ζ Phe. The errors are not shown on the Hipparcos axis for CW Cephei (the hottest binary in these figures). See text for explanation.

licities from observed data. Although a few stars show an incompatibility between the observed and synthetic $uvby$ colours if we try to match the three Strömgren indices $(b-y)$, m_1, and c_1, the overall determinations are satisfying. Moreover, an acceptable solution is always possible when only considering two photometric indices, as in Case 1 or Case 2 (see Table 3). The large range of $[Fe/H]$ associated with acceptable confidence levels makes it evident that the classical method to derive T_{eff} from metallicity-independent calibrations should be considered with caution. We found that, even for hot stars for which we expect optical photometry to be nearly insensitive to the stellar metal-content, a change in the assumed metallicity can lead to a significant change in the predicted effective temperature range. Furthermore, for cool stars, both T_{eff} and $[Fe/H]$ can be estimated with good accuracy from the photometric method. The effects of surface gravity and interstellar reddening have also been carefully studied. In particular, an apparently minor error in reddening can change dramatically the shape of the confidence contour levels, and, therefore, the parameter values

hence derived. By exploring the best χ^2-fits to the photometric data, we have re-derived new reddening values for some stars (see Table 1). Finally, comparisons for 16 stars with Hipparcos-based T_{eff} determinations show good agreement with the temperatures derived from the BaSeL models. The agreement is even excellent for the star having the most reliable Hipparcos data in the sample studied in this paper. These comparisons also demonstrate that, while originally calibrated in order to reproduce the broad-band (UBVRIJHKL) colours, the BaSeL models also provide reliable results for medium-band photometry such as the Strömgren photometry. This point gives a significant weight to the validity of the BaSeL library for synthetic photometry applications in general.

References

Andersen J., 1991, A&AR 3, 91

Andersen J., Clausen J.V., 1989, A&A 213, 183

Andersen J., Clausen J.V., Giménez A., 1993, A&A 277, 439

Andersen J., Clausen J.V., Nordström B., 1984, A&A 134, 147

Clausen J.V., 1991, A&A 246, 397

Clausen J.V., Giménez A., 1991, A&A 241, 98

Clausen J.V., Giménez A., Scarfe C., 1986, A&A 167, 287

Crawford D.L., 1973,In: Hauck B., Westerlund B.E. (eds.) IAU Symp. 54. Reidel, Dordrecht, p. 93

Crawford D.L., 1975, AJ 80, 955

Crawford D.L., 1978, AJ 83, 48

Davis J., Shobbrook R.R., 1977, MNRAS 178, 651

Edvardsson B., Andersen J., Gustafsson B., Lambert, D.L., Nissen P.E., Tomkin J., 1993, A&A 275, 101

Flower P.J., 1996, ApJ 469, 355

Grosbøl P., 1978, A&AS 32, 409

Hauck B., Mermilliod M., 1980, A&AS 40, 1

Hayes D.S., 1978, In: Davis Philip A.G., Hayes D.S. (eds.) The HR diagram. IAU Symp. 80, Reidel, Dordrecht, p. 65

Henry T.J., Mc Carthy D.W., 1993, AJ 106, 773

Hrivnak B.J., Milone E.F., 1984, ApJ 282, 748

Jakobsen A.M., 1986, Ph.D. Thesis, Aarhus Univ., Denmark

Jordi C., Ribas I., Torra J., Giménez A., 1997, A&A 326, 1044

Kurucz R., 1991, In: Davis Philip A.G., Upgren A.R., Janes Schenectady K.A. (eds.) Precision Photometry: Astrophysics of the Galaxy. L. Davis Press Inc., NY, p. 27

Lacy C.H., Frueh M.L., 1985, ApJ 295, 569

Lastennet E., 1998, Ph.D. Thesis, Obs. Astronomique de Strasbourg, France

Lastennet E., Lejeune T., Valls-Gabaud D., 1996, ASP Conf. Ser. Vol.90, 157

Lastennet E., Valls-Gabaud D., 1998, A&A, submitted

Lejeune T., Cuisinier F., Buser R., 1997, A&AS 125, 229

Lejeune T., Cuisinier F., Buser R., 1998a, A&AS 130, 65

Lejeune T., Westera P., Buser R., 1998b (BaSeL models), in preparation

Lutz T.E., Kelker D.H., 1973, PASP 85, 573

Magain P., 1987, A&A 181, 323

Moon T.T., Dworetsky M.M., 1985, MNRAS 217, 305

Morton D.C., Adams T.F., 1968, ApJ 151, 611

Napiwotzki R., Schönberner D., Wenske V., 1993, A&A 268, 653

Osmer P.S., Peterson D.M., 1974, ApJ 187, 117

Popper D., 1980, A&AR 18, 115

Popper D., 1987, AJ 93, 672

Popper D., Andersen J., Clausen J.V., Nordström B., 1985, AJ 90, 1324

Pols O.R., Tout C.A., Schröder K.-P., Eggleton P.P., Manners J., 1997, MNRAS 289, 869

Relyea L.J., Kurucz R.L., 1978, ApJS 37, 45

Ribas I., Giménez A., Torra J., Jordi C., Oblak E., 1998, A&A 330, 600

Saxner M., Hammarbäck G., 1985, A&A 151, 372

Schmidt-Kaler, 1982, In: Schaifers K., Voigt H.H. (eds.) Landolt-Börnstein. Neue Serie, Gruppe VI, Bd. 2b, Springer, Berlin, p. 14